

Thermal Analysis of the Air Inside a Rolling Deformed Torus

Youn J. Kim*

(Received March 27, 1997)

A theoretical model has been developed for calculating the internal temperature distribution and its associated heat flux in a deformed torus while free rolling under load. With the pure-conduction limit, the analytic expression for the heat transfer rate predicted by this model is derived. Analytical results show that the distributions of temperatures and heat transfer rates in a rolling deformed torus are strongly influenced by the thermal boundary conditions at the inner and outer tire surfaces. Also, the results of present study match quite closely with those found by Wey in the region away from the footprint.

Key Words : Rolling Tire, Nusselt Number, Poisson Integral

Nomenclature

a	: Undeformed cross-sectional radius of torus	$x, y, z (\xi, \eta, \zeta)$: Cartesian (dimensionless) coordinates
C_p, C_v	: Specific of heat at constant pressure and volume, respectively	α	: Thermal diffusivity of air ($\equiv k/\rho C_v$)
c	: Wall velocity in the z -direction	γ	: Specific heat ratio
h	: Heat transfer coefficient	δ_{\max}	: Maximum radial displacement of the deformed torus
k	: Thermal conductivity of air	μ	: Fluid viscosity
L	: Half length of the deformed region	ν	: Fluid kinematic viscosity
Nu	: Nusselt number ($= h \cdot 2a/k$)	ρ	: Fluid density
Pr	: Prandtl number ($= \mu C_p/k$)	σ	: Cylindrical radius
R	: Local radius of the torus cross section	Θ	: Dimensionless temperature
r, θ, z	: Cylindrical coordinates		
Re	: Reynolds number ($= ca/\nu$)		
T	: Temperature		
v_r, v_θ, w	: Velocity components in radial (r), angular (θ), and axial (ϕ) directions		
$u, v, w (U, V, W')$: Velocity components (dimensionless) in the cartesian coordinates		
w'	: The increment in the ϕ -component of velocity		

1. Introduction

In a rolling deformed tire, mechanical energy is converted to heat during the constant flexing of the rubber. Some of this heat is conducted to the outer surface, where it is carried away by convection to the air surrounding the tire and by contact conduction to the roadway. In addition, some of the heat generated is conducted to the inside surface of the tire, where the convection carries it from the hot rubber surface to the relatively colder rim. Traditionally, the latter energy path has been neglected, since it was assumed that the inner air was in solid-body rotation, leading to an adiabatic-wall condition at the inside surface (Clark 1976).

However, hot wire anemometer measurements

* School of Mechanical Engineering, Institute of Advanced Machinery and Technology, Sung Kyun Kwan University, Suwon 440-746, Korea

of inner-air velocities reported by Schuring *et al.* (1982), were found to be on the order of ten to thirty percent of wheel speed, relative to the rubber. Subsequent measurements (Rae and Skinner 1984) provided greater detail about the velocity distributions and led to the conclusion that the heat transfer to the inner air could be competitive with that occurring on the outer surface. These measurements, along with an analytic solution for the flowfield in a very thin tire at vanishing Reynolds number (Rae 1983) served to establish the main features of the flow, which can be regarded as steady when viewed in a coordinate system translating with the wheel.

The objective of this paper seeks to extend the analysis of Kim (1997) to include the temperature distribution inside a rolling deformed torus, and to establish more realistic models of the tire cross-sectional shape. Analytic solutions for non-zero ratio of cross-sectional radius to wheel radius appear to be a much more difficult problem, because the governing equations are fully three-dimensional, in addition to the complications already mentioned by Kim. Numerical solutions of the complete equations have been reported in Taulbee *et al.* (1984) and Wey (1985) for Reynolds numbers up to 100.

The basic equations and approximations made are presented in Sec. 2. Then, the temperature field and its associated heat flux are considered in Sec. 3, where the tire is modelled as having a given distribution of surface temperature: uniformly hot on a portion representing the tread, uniformly cold on a portion representing the rim, and having a linear and sinusoidal distributions of temperature between these extremes, on the portions representing the sidewalls. For these temperature distributions, there is a flow of heat even in the absence of torus deformation or induced air flow; the heat transfer distribution in this case amounts to a calculation of the shape factor for pure-conduction through a static medium in a differentially heated toroid.

For small values of the radius ratio, the tire geometry approaches that of a pipe whose axis is straight, but whose cross-section is deformed. In this limit, analytic solutions can be found in two

cases: the first applies at small Reynolds number, where the appropriate equations are those of Stokes flow, and reduce to Poiseuille flow when the deformation is small enough that the longitudinal components of the shear stress are negligible in comparison to the traverse ones. This limit is discussed in Sec. 3, along with the modifications that are caused by the inner air flow when the torus is deformed.

The problem of finding the distribution of the rubber temperature in an actual tire is much more complex. It is necessary to consider in detail the mechanics of the deformation and distribution of volumetric heat generation, in addition to the distribution of the heat transfer coefficients (Trivisonno 1970, McCarty 1982). The present work is an attempt to shed some light on only the last of these, and is an essential first step in clarifying both the magnitude and the basic mechanics of the internal-air energy-conduction path.

2. Formulation of Problems

The energy equation, assuming constant thermal properties and neglecting dissipation, has the following form in the Dean coordinates:

$$\begin{aligned}
 &v_r \frac{\partial T}{\partial r} + \frac{v_\theta}{r} \frac{\partial T}{\partial \theta} + \frac{w}{\sigma} \frac{\partial T}{\partial \phi} \\
 &= \alpha \left\{ \frac{\partial^2 T}{\partial r^2} + \frac{1}{r} \frac{\partial T}{\partial r} + \frac{1}{r^2} \frac{\partial^2 T}{\partial \theta^2} \right. \\
 &\quad \left. + \frac{\cos \theta}{\sigma} \left(\frac{\partial T}{\partial r} - \frac{1}{r} \frac{\partial T}{\partial \theta} \right) + \frac{1}{\sigma^2} \frac{\partial^2 T}{\partial \phi^2} \right\}
 \end{aligned} \tag{1}$$

where T is the temperature, $\alpha \equiv k/\rho C_v$ is the thermal diffusivity of air, k and C_v being the thermal conductivity of air and specific heat at constant volume. The cylindrical radius is denoted by σ , while v_r , v_θ and w denote the velocity components in the r , θ and ϕ directions, respectively. For some purpose it is useful to separate the solid-body rotation parts of the ϕ -component of the velocity, as follows:

$$w = \Omega \sigma + w' \tag{2}$$

where Ω denotes the angular velocity of rotating torus.

Consider now a pipe whose undeformed cross-

sectional scale is a , and has a deformed region of length $2L$ and maximum deflection δ_{\max} (see Fig. 1). The velocity of the wall in the z -direction is called c . The appropriate energy equation with the thin-tire limit can then be written in the cartesian-coordinate form by letting the cross-sectional radius r be small in comparison to the wheel radius R , as follows :

$$u \frac{\partial T}{\partial x} + v \frac{\partial T}{\partial y} + w \frac{\partial T}{\partial z} = \alpha \left\{ \frac{\partial^2 T}{\partial x^2} + \frac{\partial^2 T}{\partial y^2} + \frac{\partial^2 T}{\partial z^2} \right\} \quad (3)$$

where $z = R(\phi - \pi)$ lies along the axis of the channel, while x and y lie in the cross-sectional shape. Here, R is the fixed radial location of some convenient point in the tire cross section, such as its centroid in the undeformed state. The coordinates and velocities are now made dimensionless, as follows :

$$\begin{aligned} \xi &= x/a, \quad \eta = y/a, \quad \zeta = z/L, \\ U &= \frac{L}{\delta_{\max}} \frac{u}{c}, \quad V = \frac{L}{\delta_{\max}} \frac{v}{c}, \\ W' &= \frac{L}{\delta_{\max}} \left(\frac{w}{c} - 1 \right) \end{aligned}$$

and a dimensionless temperature is introduced as

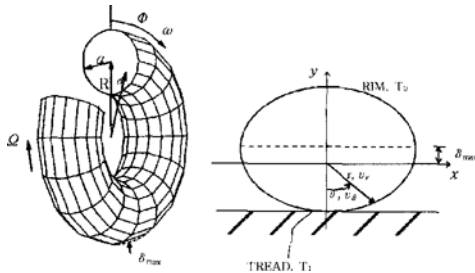


Fig. 1 Toroidal coordinates system.

$$\Theta \equiv \frac{T - T_o}{T_1 - T_o}$$

where T_o and T_1 are the temperatures to be assigned to the rim and tread portions of the tire surface, respectively. This leads to

$$Re \frac{\delta_{\max}}{L} \left(U \frac{\partial \Theta}{\partial \xi} + V \frac{\partial \Theta}{\partial \eta} \right) + Re \frac{a}{L} \left(1 + \frac{\delta_{\max}}{L} W' \right) \frac{\partial \Theta}{\partial \zeta} = \frac{\gamma}{Pr} \nabla^2 \Theta \quad (4)$$

where

$$\nabla^2 \equiv \frac{\partial^2}{\partial \xi^2} + \frac{\partial^2}{\partial \eta^2} + \left(\frac{a}{L} \right)^2 \frac{\partial^2}{\partial \zeta^2}$$

$$Re \equiv \frac{ca}{\nu}, \quad \gamma = C_p / C_v, \quad Pr \equiv \mu C_p / k$$

The Poiseuille-flow limit is now found by taking $Re \rightarrow 0$, $a/L \rightarrow 0$; the velocities and the temperature are expanded in powers of a/L :

$$\begin{aligned} W' &= W'_o + \frac{a}{L} W'_1 + \mathcal{O}(a/L)^2 \\ U &= \frac{a}{L} U_1 + \mathcal{O}(a/L)^2 \\ V &= \frac{a}{L} V_1 + \mathcal{O}(a/L)^2 \\ \Theta &= \Theta_o + \frac{a}{L} \Theta_1 + \mathcal{O}(a/L)^2 \end{aligned} \quad (5)$$

Then the equations to be solved for the zeroth- and first-orders are

$$\left(\frac{\partial^2}{\partial \xi^2} + \frac{\partial^2}{\partial \eta^2} \right) \Theta_o = 0 \quad (6)$$

$$Re \frac{\partial \Theta_o}{\partial \zeta} = \frac{\gamma}{Pr} \left(\frac{\partial^2}{\partial \xi^2} + \frac{\partial^2}{\partial \eta^2} \right) \Theta_1 \quad (7)$$

The boundary conditions are that Θ_o varies between 0 and 1 over prescribed portions of the surface, while Θ_1 is zero on the boundary.

Table 1 Various thermal boundary conditions for the undeformed portion of the torus.

CASE	A (Wey 1985)	B	C
$0 \leq \theta \leq \pi/4$ $7\pi/4 \leq \theta \leq 2\pi$	1	$\frac{1}{2}(1 + \cos\theta)$	1
$3\pi/4 \leq \theta \leq 5\pi/4$	0		0
$\pi/4 \leq \theta \leq 3\pi/4$	$1 - \frac{\theta - \pi/4}{\pi/2}$		$\frac{1}{2} \left[1 + \cos 2 \left(\theta - \frac{\pi}{4} \right) \right]$
$5\pi/4 \leq \theta \leq 7\pi/4$	$\frac{\theta - 5\pi/4}{\pi/2}$		$\frac{1}{2} \left[1 - \cos 2 \left(\theta - \frac{\pi}{4} \right) \right]$

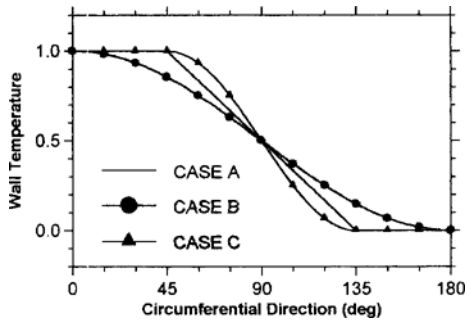


Fig. 2 Various wall temperature distributions for the pure-conduction limit as shown in Table 1.

The leading term in the temperature is the pure-conduction limit, while the first convection involves only the solid-body portion of the flow-field (i. e., the c in Re on the left-hand side of the equation for θ_1) and also involves the ζ -variations in θ_o that are due to the deflected geometry. It is interesting that neither the primary nor the secondary velocities (W_o' , U_1 , V_1) affect the temperature field, to this order.

The pure-conduction term θ_o has been calculated for the undeformed portion of the torus, and for the different boundary conditions as shown in Table 1.

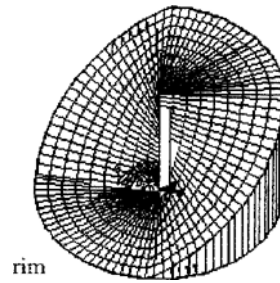
In order to elucidate the effects of wall temperature distributions on the heat transfer rates in a rolling deformed torus, these different boundary conditions are used. Figure 2 shows the above wall temperature distributions for the pure-conduction limit.

3. Results and Discussion

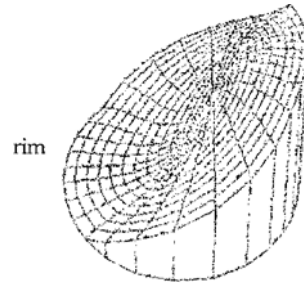
The above limiting case can be easily calculated, using Poisson's integral. The distribution of temperature at all points (r , θ) in a cylindrical volume with a given distribution of surface temperature is given by (Carslaw and Jaeger 1980) :

$$\theta(r, \theta) = \frac{1}{2\pi} \int_0^{2\pi} \frac{\Theta(a, \lambda) (a^2 - r^2)}{a^2 + r^2 - 2ar \cos(\lambda - \theta)} d\lambda \tag{8}$$

The curvature and deformation of the tire volume are neglected at this level of approximation.



(a) Present study



(b) Three-dimensional numerical study (adapted from Wey, 1985)

Fig. 3 Temperature profiles at the cross-section of the tire with $\phi=180^\circ$.

The calculated results of the distribution of temperature profiles at the cross-section of the tire with $\phi=180^\circ$ are compared with the results taken from Wey (1985), and presented in Fig. 3. It should be noted that the code used in Wey are the three-dimensional one. In interpreting these results it should be kept in mind that between $\phi=150^\circ$ and 180° the secondary flows moves toward rim, as described in Wey. The effects of secondary flow shifting hot air from outer wall (bottom) to the area between the center and outer wall can be seen.

The corresponding heat transfer rate, expressed in terms of a heat transfer coefficient h , is

$$q'' = k \frac{\partial T}{\partial r} \Big|_{r=a} \equiv h(T_1 - T_o) = k(T_1 - T_o) \frac{\partial \theta}{\partial r} \Big|_{r=a} \tag{9}$$

Thus the Nusselt number is defined as

$$Nu \equiv \frac{h \cdot 2a}{k} = 2 \frac{\partial \theta}{\partial (r/a)} \Big|_{r/a=1} \tag{10}$$

A positive value of Nu corresponds to heat trans-

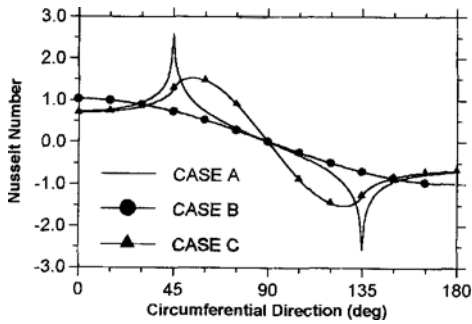


Fig. 4 Heat transfer rates for the pure-conduction limit with different boundary conditions of wall temperature distributions as given in Table 1.

fer from the wall to the gas, and conversely. Figure 4 shows a numerical evaluation of this quantity with different boundary conditions of wall temperatures; Poisson's integral was used to calculate Θ at $r=0.99a$, and the radial gradient can then be evaluated, for example by forming the difference of the temperature at a radius just inside the wall and the temperature of the wall, divided by the increment in radius

$$\frac{\partial \Theta}{\partial (r/a)} = \frac{\Theta_{(r/a=1)} - \Theta_{(r/a=0.99)}}{0.01} \quad (11)$$

The evaluations of Poisson's integral were done by the Simpson rule, using $\Delta\lambda=0.5^\circ$. The results of Nusselt number distribution with the thermal boundary condition A, shown in Fig. 4, match quite closely with those found by Wey (1985) in the region away from the footprint. Figure 5 adapted from Wey's thesis shows how this Nusselt number is distributed over the inside surface of the tire. Actually, the exact analytic evaluation of the Poisson integral would yield logarithmic singularities at the positions where the slope of the wall temperature versus angular position is discontinuous, but this detail is not worth pursuing, for the level of approximation being used here. (The peaks in this distribution are analytically, logarithmic singularities, but are assigned finite values by the numerical evaluation).

Of principal interest here is the net heat transfer to the wall, per unit distance along the tire :

$$\bar{q}' \equiv \frac{\int q'' dA}{dz} = a \int_0^{2\pi} q'' d\theta$$

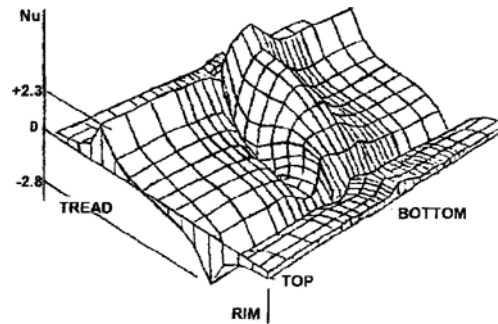


Fig. 5 Heat transfer distributions (adapted from Wey, 1985).

$$= \frac{k(T_1 - T_0)}{2} \int_0^{2\pi} Nu d\theta \quad (12)$$

For the results shown in Fig. 4, this integrated heat transfer rate has the following values with different thermal boundary conditions

$$\frac{2\bar{q}'}{k(T_1 - T_0)} = \begin{cases} +3.802317 & \text{for CASE A} \\ +4.196146 & \text{for CASE B} \\ +3.805207 & \text{for CASE C} \end{cases} \quad (13)$$

The positive sign indicates a net heat transfer from the hot portion of the wall to the cold portion.

4. Conclusions

The structure of the temperature field in the inner air and the distribution of heat transfer rates over the inner surface are studied analytically with the pure-conduction limit. Results of these analyses show that the distributions of temperatures and heat transfer rates are strongly influenced by the thermal boundary conditions at the inner and outer tire surfaces. These results are compared with those found by Wey (1985) and reasonable agreement is obtained in the region away from the footprint.

For better understanding of the fluid-mechanical and thermal behaviour of this fascinating flow problem, however, it may be necessary to perform the experimental works. In the near future we would be glad to compare these theoretical results with those obtained by anyone in the same field.

References

- Carslaw, H. S. and Jaeger, J. C., 1980, *Conduction of Heat in Solids*, 2nd ed., Oxford, Clarendon Press
- Clark, S. K., 1976, "Temperature Rise Times in Pneumatic Tires," *Tire Science and Technology*, Vol. 4, No. 3, pp. 181~189.
- Kim, Y. J., 1997, "Analytic Solutions of Flow-fields Inside a Rolling Deformed Torus," *KSME Int. J.*, Vol. 11, No. 1, pp. 67~76.
- McCarty, J. L., 1982, "Results from Recent NASA Tire Thermal Studies," *Tire Modeling, NASA CP 2264*, pp. 211~222.
- Rae, W. J., 1983, "Flow Inside a Pneumatic Tire : A Peristaltic-Pumping Analysis for the Thin-Tire Limit at Very Low Forward Speed," *J. of Applied Mechanics*, Vol. 105, pp. 255~258.
- Rae, W. J. and Skinner, G. T., 1984, "Measurements of Air Flow Velocity Distributions Inside a Rolling Pneumatic Tire," *SAE Paper 840066*
- Schuring, D. J., Skinner, G. T. and Rae, W. J., 1982, "Contained Air Flow in a Radial Tire," *SAE Transactions*, Vol. 90, pp. 705~712.
- Taulbee, D. B., Wey, M. J. and Rae, W. J., 1984, "Calculation of Flow Inside a Loaded Rotating Tire," *the 37th Annual Meeting, American Physical Society, Division of Fluid Dynamics*, Providence, RI.
- Trivisonno, N. M., 1970, "Thermal Analysis of a Rolling Tire," *SAE Paper 700474*.
- Wey, M. J., 1985, "Numerical Simulation of Flow Inside a Loaded Rotating Tire." Ph. D. Dissertation, State Univ. of New York at Buffalo.